Accepted Manuscript

Third-harmonic generation via rapid adiabatic passage based on gradient deuterium $KD_xH_{2-x}PO_4$ crystal

Lailin Ji [1, †, *], Li Yin [1, 2, †], Jinsheng Liu [1, †], Xianghe Guan [1], Mingxia Xu [3], Xun Sun [3], Hao Xu [1], Wei Feng [1], Dong Liu [1], Ruijing He [1], Tianxiong Zhang [1], Yong Cui [1], Xiaohui Zhao [1], Yanqi Gao [1], and Zhan Sui [1]

[1] *Shanghai Institute of Laser Plasma, China Academy of Engineering Physics, Shanghai 201800, China*

[2] *Key Laboratory on High Power Laser and Physics, Shanghai Institute of Optics and Fine Mechanics, Chinese Academy of Sciences, Shanghai 201800, China*

[3] *Key State Key Laboratory of Crystal Materials, Shandong University, Jinan 250100, China*

[†] *These authors contributed equally to this work.*

Abstract Broadband frequency-tripling pulses with high energy are attractive for scientific research such as inertial confinement fusion (ICF), but are difficult to scale up. Third-harmonic generation (THG) via nonlinear frequency conversion, however, remains a trade-off between bandwidth and conversion efficiency. Based on gradient deuterium deuterated potassium dihydrogen phosphate ($KD_xH_{2-x}PO_4$, DKDP) crystal, here, we report the generation of frequency-tripling pulses by rapid adiabatic passage (RAP) with low-coherence laser driver facility. The efficiency dependence on phase matching (PM) angle in Type-II configuration is studied. We attained an output at 352 nm with a bandwidth of 4.4 THz and an efficiency of 36%. These results, to the best of our knowledge, represents the first experimental demonstration of gradient deuterium DKDP crystal in obtaining frequency-tripling pulses. Our research paves a new way for developing high-efficiency, large-bandwidth frequency-tripling technology.

10.1017/hpl.2024.90

Key words: *Third-harmonic generation; Gradient deuterium DKDP crystal; Rapid adiabatic passage; Nonlinear frequency conversion.*

*Correspondence to: Lailin Ji, Shanghai Institute of Laser Plasma, China Academy of Engineering Physics, Shanghai 201800, China. Email: jsycjll@siom.ac.cn

I. Introduction

THG source from Nd:glass laser driver facility has become an ideal wavelength for ICF. Accurately, THG light source in conjunction with broad bandwidth, can effectively suppress laser plasma instability (LPI) issues [1-2], making it crucial for the successful ignition of laser driven ICF. Quadratic nonlinear frequency conversion, including second-harmonic generation (SHG) and sum-frequency generation (SFG), is a direct route for converting fundamental light pulses into the THG region [3-4]. Babushkin et al. validated the two-crystal cascade scheme by SFG, achieving a THG bandwidth of up to 1.1 THz@351 nm [5-6]. Dorrer et al. proposed a novel method using grating angular dispersion compensation, combined with broadband and narrowband SFG to achieve a THG bandwidth of 10 THz@351 nm [7]. While these schemes have successfully generated broadband THG, the former is constrained by the THG efficiency, which is quite sensitive to the spacing between the two mixers, and the latter is limited by the damage threshold of ultraviolet gratings, making it difficult to widely promote application. Therefore, how to efficiently obtain broadband THG light sources with robustness is a crucial issue that needs to be addressed urgently.

Nonlinear frequency conversion, a widely-used route for THG, however faces a trade-off between bandwidth and conversion efficiency [8-9]. Essentially, it involves managing populations numbers within an inhomogeneous quantum two-state system. The same issue also arises in quantum two-level systems with an global inhomogeneity: the non-uniform resonant frequency limits the complete population inversion or any alternative required quantum state preparation to

https://doi.org/10.1017/hpl.2024.90 Published online by Cambridge University Press

a small part of ensemble. The solution has long been established [10-12]: as for nuclear magnetic resonance and atoms or molecules, RAP [13] produces violent particle number inversion without precise integration of power electromagnetic coupling pulses, effectively overcoming the impurities in the preparation of quantum states in non-uniform ensembles. Fortunately, it is noted that RAP in parametric three-wave mixing process, analogous to the two-level quantum system, can overcome the trade-off and achieve high-efficient frequency conversion with a broad bandwidth [14-15]. Here, the phase mismatch gradually varies from a significant negative (positive) to positive (negative) value as the interaction unfolds. The RAP system should ideally start and finish near a stationary state in which the nonlinear coupling is negligible, suggesting a robust performance.

The adiabatic THG process essentially involves the regulation of refractive index characteristics of the crystal to satisfy the RAP conditions [16]. The reported regulation methods mainly focus on the application of external fields, including temperature [17] and electric fields [18]. These two methods, however, are easily affected by external perturbations. One expected approach is to perform gradient-doping concentration inside the nonlinear crystal to modify its refractive index, thereby permanently altering the intrinsic properties of the crystal without external field control. In our previous theoretical work, we utilized gradient-doping crystals to adiabatic THG process and formulated a comprehensive technical scheme. In this work, we present an experimentally demonstration of a gradient-doped crystal in the generating frequency-tripling pulse through RAP by a nanosecond laser, which represents the current state of the art in this field. A compact THG setup and a high-efficiency THG architecture was tested, respectively. The former achieved an efficiency of 7%, while the latter, which was equipped with a narrowband fundamental

https://doi.org/10.1017/hpl.2024.90 Published online by Cambridge University Press

laser, reached an efficiency of 36%. These results demonstrate the superiority of RAP-based frequency-tripling in terms of incident angle tolerance, high efficiency and broad bandwidth.

II. RAP based on gradient deuterium DKDP crystal

To date, with 1 μm lasers, typical oxide crystals of β-BaB_2O_4 [19-20], $CsLiB_6O_{10}$ [21-22], LiB_3O_5 [23-24] or KH_2PO_4 (KDP) [25-26] have been widely applied in up- and down-frequency conversion. KDP crystals, notably for their capability to grow large-sized, high-quality single crystals, possess distinctive advantages in the THG process. It has been demonstrated that KDP can be extensively applied for THG driven by high-power laser [27-28]. We intend to implement the gradient-doping strategy in KDP crystals and demonstrate its potential in THG.

In contrast to KDP with a fixed doping concentration, Mingxia Xu et.al from Shandong University has successfully grown KDP crystals doped with a gradient deuterium [Figure 1(a)] through a "point-seed" rapid growth method in a 5 L container [29]. Within the crystal, the deuterium concentration increases linearly along the beam propagation direction. The amount of doping deuterium directly affects the properties of refractive index in KDP crystal, and the refractive index is varied with the doping deuterium given in the formula: $n^2(x) = xn_D^2 + (1-x)n_H^2$, where n represents the refractive index of deuterium-doped crystal, n_D is the refractive index of fully doped deuterium, n_H corresponds to the refractive index of a deuterium-free KDP crystal, and x denotes the doping-deuterium along the optical axis.

Gradient deuterium DKDP crystal has remarkable potential in high-efficiency THG wherein adiabatic schemes are especially attractive for their robustness to small changes in parameters that affect the phase evolution of the process. Analogous to adiabatic mechanism in two-level quantum systems, the phase mismatch parameter should vary slowly during the

https://doi.org/10.1017/hpl.2024.90 Published online by Cambridge University Press

conversion process, from a large negative value to a large positive one or vice versa. In the presence of a sufficiently strong pump field, as for SFG, energy is efficiently converted from lower to higher frequency. Thus, adiabatic scheme relaxes the restriction of minimizing the phase mismatch between the interacting beams, and instead requires Δk to be varied slowly during frequency conversion. The adiabatic conditions can be written as [30-32]:

$$\left|\frac{d\Delta k}{dz}\right| << \frac{\left(\Delta k^2 + \kappa^2\right)^{3/2}}{\kappa} \tag{1}$$

where $\Delta k = k_1 + k_2 - k_3$ represents the phase mismatch among the interacting waves, k_1, k_2 and k_3 refer to the wave-number of the seed, pump and generated frequency, respectively. z is the position along the propagation direction. κ is the coupling coefficient and equals to $\kappa = \frac{4\pi w_1 w_3}{\sqrt{k_1 k_3 c^2}} \chi^{(2)} A_2$, where w_1 and w_3 are the frequencies of seed and generated. c is the light speed in vacuum, A_2 is the pump amplitude and $\chi^{(2)}$ is the second-order susceptibility of the crystal.

The violent phase mismatch within the crystal, near the entrance and exit of the crystal, were employed to handle the inherent trade-off of adiabatic process [Figure 1(b)]. The RAP should ideally start and end near a stationary state where we can neglect the nonlinear coupling. We emphasize that the eigenstate at the exit of the crystal is quite different from that of the entrance. For SFG, all light is at the initial state whereas, at the final state, 40% light is at the third-harmonic [Figure 1(c)]. Meanwhile, the stationary state needs to vary very slowly by changing phase mismatch, in order to remain an eigenstate of the evolving system as it passes through the PM concentration.

https://doi.org/10.1017/hpl.2024.90 Published online by Cambridge University Press

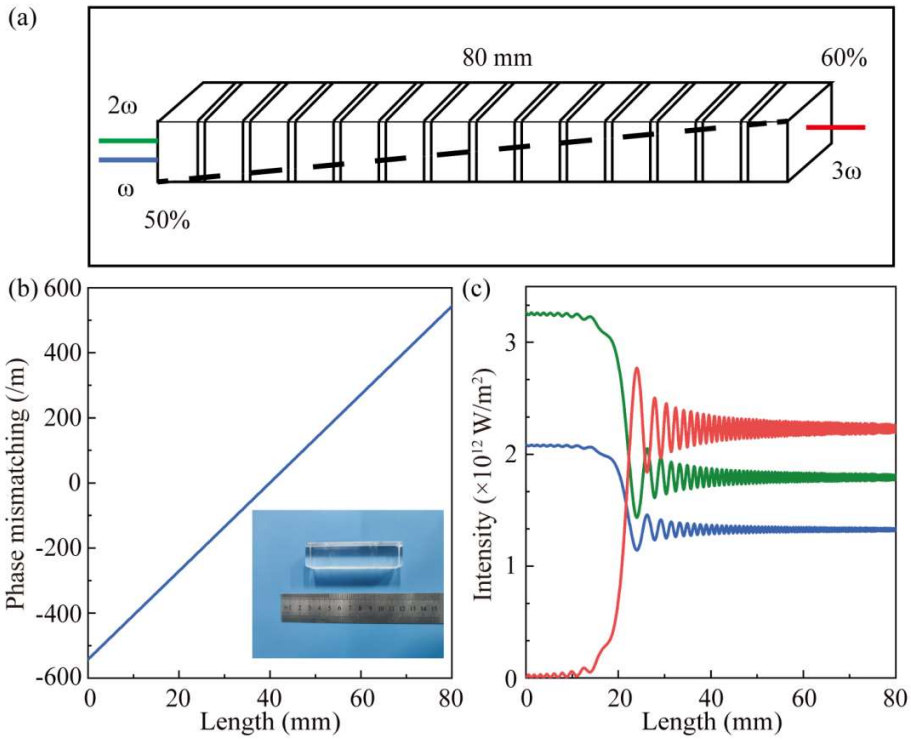

Figure 1. (a) The diagram of gradient deuterium DKDP. A high-quality Type-II PM direction gradient deuterium DKDP crystal with dimensions of 20×20×80 mm is employed in the THG scheme. The deuterium content ranges from 50% to 60% with a change of 10% in an 80-mm-thickness crystal and maintains 55% at the center of the crystal. (b) The variation of phase mismatch in SFG as a function of crystal length. The calculations assumed a monochromatic light of frequency mixing at 1058 nm, 529 nm and 352 nm, respectively. Insert: The photo of gradient deuterium DKDP crystal. (c) Intensity evolution for SFG of the fundamental frequency (blue), second- (green) and third- (red) harmonics. The input broadband fundamental frequency light has an intensity of 0.8 GW/cm^2. Assuming the total transmission loss before the KDP crystal is 20% and the efficiency of broadband SHG with KDP is 50%. Therefore, the intensity broadband SHG is about 3.2×10^{12} W/m^2 and the given narrowband intensity is comparable to the SHG.

III. Experimental scheme and results

3.1 SHG source architecture

The experimental setup is schematically shown in Figure 2(a). The pump source is a low-coherence broadband laser [33-36] that generates 4 ns pulses at 1058 nm, with an output energy

https://doi.org/10.1017/hpl.2024.90 Published online by Cambridge University Press

up to 500 mJ. After a 1:3 beam telescope, the diameter of beam profile from the broadband pump source is 5 mm, and the input bandwidth (FWHM) can reach 10 nm. The crystal temperature and incident angle are critical parameters that directly affect the efficiency and stability of nonlinear frequency conversion. A KDP crystal with thickness of 18 mm, cut at $\theta = 41.1°$ and $\varphi = 45°$ for Type-I ($o_{1w}+o_{1w}\rightarrow e_{2w}$) PM, is used in the SHG stage at room temperature (Note that: all crystals employed in our experiment are equipped with anti-reflection-coated for the corresponding wavelength). The effective nonlinear coefficient of KDP was $d_{36}\sin\theta\sin2\varphi$ (Type-I) or $d_{36}\sin2\theta\cos2\varphi$ (Type-II), where d_{36}=0.38 pm/V [37-38].

Next, we reported the experimental results of SHG. The pulse profile for SHG (green) and fundamental frequency (blue) are shown in Figure 2(b) and the Insert. We demonstrated the conversion efficiency [Figure 2(c)] as a function of PM angle for Type-I SHG at a fundamental frequency energy of 40 mJ. The conversion efficiency for both SHG and THG, according to the Manley-Rowe relationship, is defined as the ratio of generated pulse energy to total incident energy. We controlled the PM angle by a high-precision rotary stage where the minimum scale value is 0.02 mrad. The efficiency is very sensitive to the PM angle, which is tuned from -4.18 to -4.46 mrad, reaching a maximum efficiency ~15.7% at -4.32 mrad. We conducted the experiment of generated spectrum under the largest SHG efficiency condition. After a KDP-based SHG stage, 90% of the energy corresponds to a bandwidth of approximately 5 nm with a central wavelength at 528.2 nm.

https://doi.org/10.1017/hpl.2024.90 Published online by Cambridge University Press

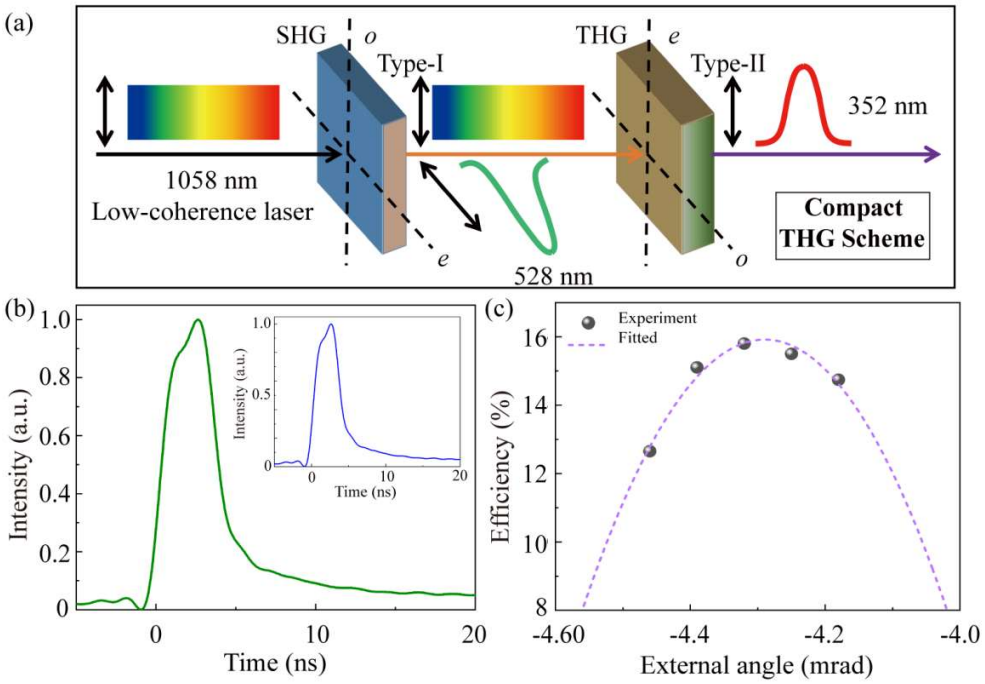

Figure 2. (a) Schematic setup of compact THG based on low-coherence broadband laser. The optical axis of SHG (THG) crystal is located in the horizontal (vertical) plane. (b) Pulse profile for SHG (green). Insert: Pulse profile for fundamental frequency (blue). (c) SHG efficiency is varied with external angle (black dots) and its quadratic-polynomial fit (purple curve).

3.2 Compact THG configuration

We carried out a compact THG experiment under an output SHG pulse energy of 100 mJ, shown in Figure 2(a). The broadband SHG light output from the KDP crystal and the residual broadband fundamental light directly achieved nonlinear frequency conversion process to generate third harmonic. Different from SHG crystal, the optical axis of THG crystal is located in the vertical plane and we need to adjust the angle vertically. Only Type-II (e_{1w}+o_{2w}→e_{3w}) PM is studied for THG due to a slightly minimized group-velocity mismatch (GVM). When the angle of controlled stage varied from 2.48 mrad to 17.74 mrad, the conversion efficiency of THG process is insensitive, which is due to the angular tolerance of the gradient deuterium DKDP crystal. As shown in Figure 3, the angle bandwidth (FWHM) is 15.26 mrad. Note that lower energy can avoid

https://doi.org/10.1017/hpl.2024.90 Published online by Cambridge University Press

crystal damage, and at the same time, the efficiency is more sensitive to changes in the phase matching angle, making it easier to find the optimal angle. We fixed the angle at 10.5 mrad and changed the intensity of the input broadband fundamental light. The conversion efficiency of THG also varied and achieved a maximum THG conversion efficiency of ~7.16% when the fundamental-frequency energy is about 400 mJ.

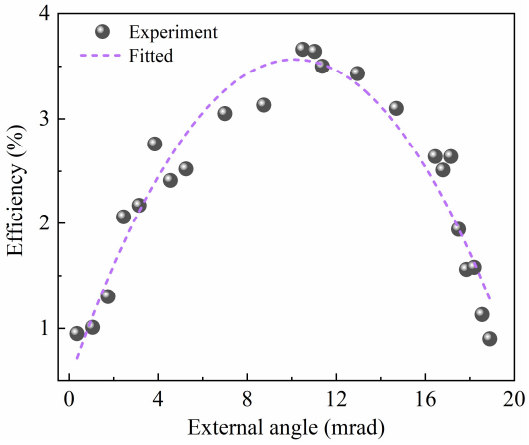

Figure 3. Dependence of tripling-efficiency on the rotation angle of the gradient deuterium DKDP crystal (black dots) and its quadratic-polynomial fit (purple curve).

3.3 High-efficiency THG architecture

To enhance the efficiency of generating broadband THG source, we combined an advanced broadband THG technology proposed by Liejia Qian with adiabatic PM process [39-41]. It is an efficient frequency-tripling scheme for 352 nm broadband pulses generation by combination of broadband and narrowband Nd:glass lasers. This scheme eliminates the need for dispersive elements such as large-aperture gratings and can be combined with gradient deuterium DKDP crystal, potentially breaking through the trade off in high efficiency and broad bandwidth. Research has found that using narrow bandwidth laser pulses can slow down the GVM effect on efficiency during nonlinear frequency conversion process of broadband lasers. Meanwhile, the

https://doi.org/10.1017/hpl.2024.90 Published online by Cambridge University Press

GVM related to narrow bandwidth lasers does not affect the PM bandwidth of THG, thereby scaling up the THG conversion efficiency of broadband lasers. Furthermore, by utilizing the large mismatch in group velocity for Type-II PM process in KDP crystal, the introduction of narrow bandwidth laser pulses during the THG process can effectively suppress the transfer of phase modulation of fundamental light to intensity modulation of generated frequency-tripling pulse, improving the uniformity and symmetry of output beam profile.

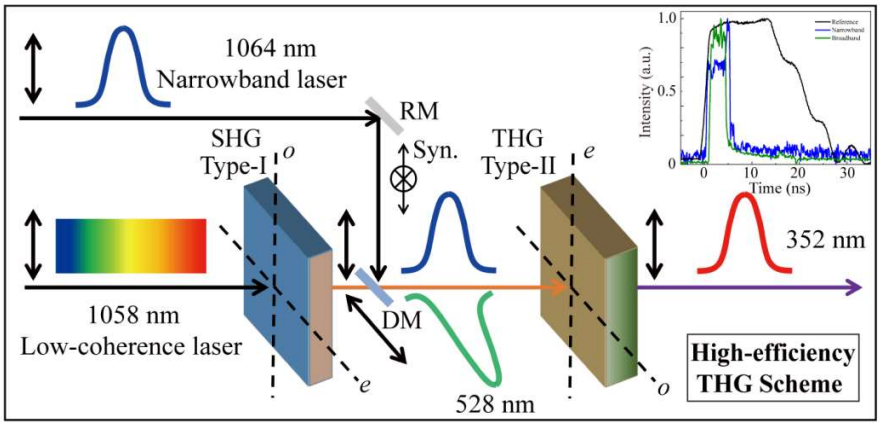

Figure 4. High-efficient schematic diagram of THG through broadband and narrowband laser sources. The optical axis of Doubler (Tripler) is also located in the horizontal (vertical) plane. Time synchronization of broadband SHG pulse (green) and narrowband fundamental frequency pulse (blue) is maintained. DM: dichroic mirror; RM: reflection mirror; Syn.: time synchronization. Insert: The black, blue and green solid line represents the reference, narrowband and broadband pulse, respectively.

The above-mentioned high-efficiency scheme for THG is shown in Figure 4. The broadband SHG source is introduced into the optical path of the THG stage after passing through a dichroic mirror (served as a short-pass filter). The narrowband fundamental light has a wavelength of 1064 nm, a pulse duration of 3 ns, and an output energy of up to 2 J. In our experiment, a reference pulse served as a time-synchronized benchmark is introduced. The leading edge of the narrowband fundamental light pulse is first aligned with that of the reference pulse.

https://doi.org/10.1017/hpl.2024.90 Published online by Cambridge University Press

Then, the pulse of the broadband frequency-doubled light is measured, and the delay is adjusted to align it with the leading edge of the reference pulse, thus achieving temporal synchronization. We measured the pulse profiles of both incident and reference beams by a photoelectric probe, as shown in Insert of Figure 4. Three front edges of pulse profiles on the oscilloscope are in aligned, making the broadband frequency-doubled light and the narrowband fundamental light synchronously incident on the frequency-tripling crystal. A zero-order half-wave plate and a polarizer at Brewster's angle with respect to the incident light were adopted to continuously attenuate the narrow-bandwidth intensity. We can successively achieve the output energy of the narrow-bandwidth through rotating the half-wave plate.

To enhance the efficiency of THG, it is essential to strictly ensure the spatial overlap of fundamental light and SHG light by precisely aligning their propagation directions. Furthermore, the conversion efficiency can also be improved if the beam aperture of the fundamental frequency light is slightly larger than that of SHG. After spatial coincidence and temporal synchronization of both the incident light, a wide-bandwidth and narrow-bandwidth SFG process is realized in a gradient deuterium DKDP crystal for Type-II configuration. We obtain a broadband THG spectrum at the center wavelength of 352.1 nm with a bandwidth of about 4.4 THz (full width at $1/e^2$ maximum), shown in Figure 5.

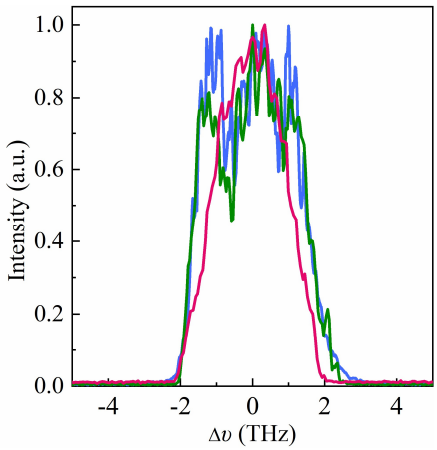

https://doi.org/10.1017/hpl.2024.90 Published online by Cambridge University Press

Figure 5. Measured spectra of fundamental frequency (blue), SHG (green) and THG (red) in high-efficiency THG scheme. The spectra are centered at 1058 nm, 528.2 nm and 352.1 nm, respectively.

Next, we demonstrate the angular robustness in our efficient frequency-tripling scheme. The energy of narrowband fundamental light was maintained at 100 mJ using an adjustable polarization system, while the energy for broadband SHG kept in 50 mJ. When the gradient deuterium DKDP crystal was tuned, the frequency-tripling efficiency reached the maximum of about 22%. The efficiencies were also monitored when tuning the angle from -2.0 mrad to 2.0 mrad, all of which exceeded 10%. The angular bandwidth is 3.78 mrad (FWHM) as shown in Figure 6(a). In comparison, using a 36-mm-thickness KDP crystal for THG, the frequency-tripling efficiency reaches its maximum of approximately 14%. The angular bandwidth is 2.66 mrad at FWHM [Figure 6(b)]. Both efficiency and angular bandwidth, obviously, were lower than those of gradient deuterium DKDP crystal. The high-efficiency frequency-tripling scheme utilizing gradient deuterium DKDP crystals exhibits angular robustness due to its adiabatic properties.

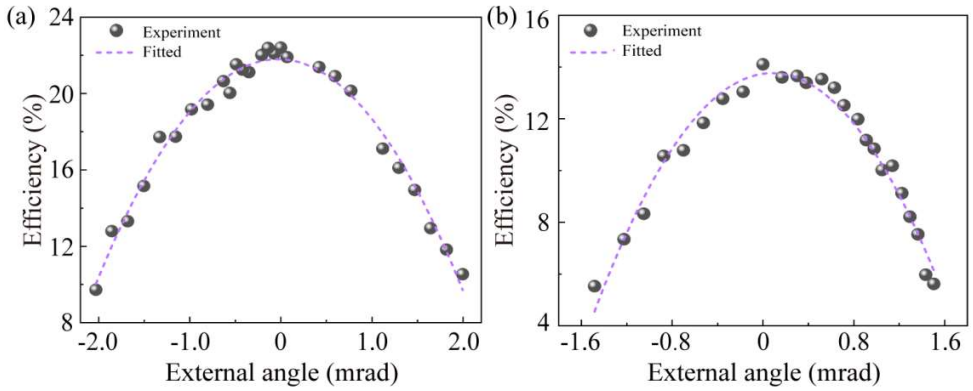

Figure 6. (a) [(b)] Conversion efficiency as a function of the crystal angular rotation for gradient deuterium DKDP crystal (KDP). The experiment data (quadratic-polynomial fit) is represented by black dots (purple curve). The energy of narrowband and broadband pulse kept in 100 mJ and 50 mJ, respectively.

https://doi.org/10.1017/hpl.2024.90 Published online by Cambridge University Press

Gradient deuterium DKDP crystals can achieve efficient broadband THG output during nonlinear frequency conversion process, achieving a conversion efficiency of 36.8% at 0.15 GW/cm^2 using the RAP [Figure 7(a)]. The energy of narrowband pulse fixed at 100 mJ in Figure 7 and the broadband pulse is 117 mJ when the conversion efficiency is 36.8%. In comparison to the compact THG configuration, the high-efficiency architectural design is capable of attaining a higher level of efficiency partially due to the incorporation of a narrowband pulse. The conversion efficiency is observed to be in close proximity to the efficiency (approximately 40%) illustrated in Figure 1(c). This experimental discrepancy can be attributed to the losses incurred during the transmission of the light beam. When broadband and narrowband fundamental frequency light are synchronously incident on a KDP crystal, broadband THG light is generated by traditional birefringent PM configuration. Figure 7 compares the adiabatic frequency conversion efficiency with that of the birefringent PM. The efficiency employed KDP is 13.7%, which is about one-third of the adiabatic frequency conversion [Figure 7(b)]. With the increase of broadband intensity @1058 nm, the efficiency of RAP process decreases slowly and remains above 30%, while that of the birefringent PM decreases faster. Different performance of efficiency evolution indicates that, to achieve maximum efficiency, a smaller amount of intensity is required in RAP process. After reaching the optimal efficiency, further increasing the injection leads to an increase of tripling energy in both RAP process and birefringent PM, but RAP has no significant efficiency backward.

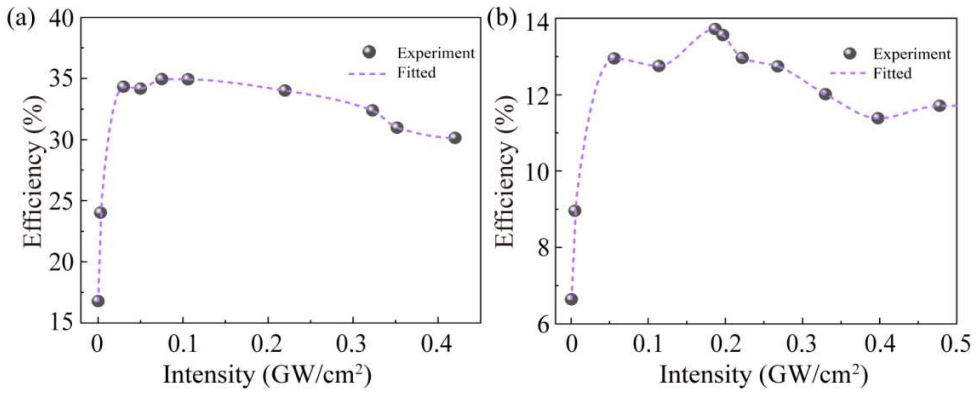

https://doi.org/10.1017/hpl.2024.90 Published online by Cambridge University Press

Figure 7. (a) [(b)] Measured efficiency as a function of broadband intensity @1058 nm for gradient deuterium DKDP crystal (KDP). Black dots and purple curve are on behalf of experimental data and quadratic-polynomial fitted curve, respectively. The energy of narrowband pulse fixed at 100 mJ.

Compared to two-crystal cascade scheme (1.1 THz@351 nm) proposed by Babushkin [5-6], we obtained a broader bandwidth of 4.4 THz. In comparison with the novel method using grating angular dispersion compensation with an efficiency of about ~8% (in the proof-of-concept experiment) [7], limited by the damage threshold of ultraviolet gratings and the beams overlap, our method can be applied to high-energy pulse while maintaining high efficiency (about 36.8%). Further more, we would like to emphasize that there is still potential for improvement in the efficiency of our experimental scheme. As the gradient deuterium DKDP crystal was newly reported in 2023, only one crystal is currently available for the THG process. In the future, crystals tailored for frequency doubler and tripler will be employed, and the adiabatic process will be applied in the entire scheme, which is expected to significantly improve efficiency and bring it close to the quantum limit.

IV. Conclusion

In summary, we have demonstrated the generation of THG in gradient deuterium DKDP crystals by RAP process. We have developed a compact THG setup that can obtain 352 nm pulses with a bandwidth of 4.4 THz, achieving an efficiency of 7%. By introducing a narrowband fundamental laser, the efficiency can be scaled up to 36%. Compared to KDP crystal, gradient deuterium DKDP crystal is a more potential candidate to generate THG due to the robustness of RAP process. The gradient deuterium DKDP combined of RAP is easy to implement and the doping profile can be reconfigured for different design parameters. We believe that these results,

https://doi.org/10.1017/hpl.2024.90 Published online by Cambridge University Press

moreover, are beyond for developing high-efficiency and broad-bandwidth lasers based on gradient-doping crystals.

Acknowledgements

This work was supported by the President Funding Independent Project of China Academy of Engineering Physics (YZJJZL2024200), National Natural Science Foundation of China (62405298) and National Key Research and Development Program (2023YFA1608503). We thank the support from Mingxia Xu and Xun Sun of Shandong University for the discussion about gradient deuterium DKDP crystals.

References

1. S. P. Obenschain, N. C. Luhmann Jr, and P. T. Greiling, "Effects of finite-bandwidth driver pumps on the parametric-decay instability," Physical Review Letters, 36, 1309 (1976). DOI: https://doi.org/10.1103/PhysRevLett.36.1309
2. R. Betti, and O. A. Hurricane, "Inertial-confinement fusion with lasers," Nature Physics, 12, 435 (2016). DOI: https://doi.org/10.1038/nphys3736
3. Y. Chen, X. Zhu, S. Ma, H. Yu, H. Wu, Z. Hu, and Y. Wu, "Effective third harmonic generation of 355 nm ultraviolet laser based on the borate-phosphate $Ba_3(ZnB_5O_{10})PO_4$

https://doi.org/10.1017/hpl.2024.90 Published online by Cambridge University Press

crystal", Optical Materials Express, 13, 3164 (2023). DOI: https://doi.org/10.1364/OME.501642

4. J. Zhao, H. Lu, J. Zheng, D. Li, Y. Zhang, X. Gan, and J. Zhao, "Strong enhancement of third harmonic generation from a Tamm plasmon multilayer structure with WS2", Optics Letters, 49, 3130 (2024). DOI: https://doi.org/10.1364/OL.524772
5. D. Eimerl, J. M. Auerbach, C. E. Barker, D. Milam, and P. W. Milonni, "Multicrystal designs for efficient third-harmonic generation", Optics Letters, 22, 1208 (1997). DOI: https://doi.org/10.1364/OL.22.001208
6. A. Babushkin, R. S. Craxton, S. Oskoui, M. J. Guardalben, R. L. Keck, and W. Seka, "Demonstration of the dual-tripler scheme for increased-bandwidth third-harmonic generation", Optics Letters, 23, 927 (1998). DOI: https://doi.org/10.1364/OL.23.000927
7. C. Dorrer, M. Spilatro, S. Herman, T. Borger, and E. M. Hill, "Broadband sum-frequency generation of spectrally incoherent pulses", Optics Express, 29, 16135 (2021). DOI: https://doi.org/10.1364/OE.424167
8. H. Suchowski, D. Oron, A. Arie, and Y. Silberberg. "Geometrical representation of sum frequency generation and adiabatic frequency conversion," Physical Review A—Atomic, Molecular, and Optical Physics 78, 063821 (2008). DOI: https://doi.org/10.1103/PhysRevA.78.063821
9. H. Suchowski, V. Prabhudesai, D. Oron, A. Arie, and Y. Silberberg, "Robust adiabatic sum frequency conversion," Optics Express, 17, 12731 (2009). DOI: https://doi.org/10.1364/OE.17.012731
10. R. P. Feynman, F. L. Vernon Jr, and R. W. Hellwarth, "Geometrical representation of the Schrödinger equation for solving maser problems", Journal of Applied Physics, 28, 49 (1957). DOI: https://doi.org/10.1063/1.1722572
11. Y. Ban, L. Jiang, Y. Li, L. Wang, X. Chen, "Fast creation and transfer of coherence in triple quantum dots by using shortcuts to adiabaticity", Optics Express, 26, 31137 (2018). DOI: https://doi.org/10.1364/OE.26.031137
12. A. Ramachandran, J. Fraser-Leach, S. O'Neal, D. G. Deppe, and K. C. Hall, "Experimental quantification of the robustness of adiabatic rapid passage for quantum state inversion in semiconductor quantum dots", Optics Express, 29, 41766 (2021). DOI: https://doi.org/10.1364/OE.435109

https://doi.org/10.1017/hpl.2024.90 Published online by Cambridge University Press

13. L. Allen, and J. H. Eberly, Optical Resonance and Two Level Atoms (Dover, New York, 1987).
14. J. Moses, H. Suchowski, and F. X. Kärtner, "Fully efficient adiabatic frequency conversion of broadband Ti: sapphire oscillator pulses", Optics Letters, 37, 1589 (2012). DOI: https://doi.org/10.1364/OL.37.001589
15. E. Bahar, X. Ding, A. Dahan, H. Suchowski, and J. Moses, "Adiabatic four-wave mixing frequency conversion", Optics Express, 26, 25582 (2018). DOI: https://doi.org/10.1364/OE.26.025582
16. H. Suchowski, G. Porat, and A. Arie, "Adiabatic processes in frequency conversion", Laser Photonics Reviews, 8, 333 (2014). DOI: https://doi.org/10.1002/lpor.201300107
17. A. Markov, A. Mazhorova, H. Breitenborn, A. Bruhacs, M. Clerici, D. Modotto, O. Jedrkiewicz, P. Trapani, A. Major, F. Vidal, and R. Morandotti, "Broadband and efficient adiabatic three-wave-mixing in a temperature-controlled bulk crystal", Optics Express, 26, 4448 (2018). DOI: https://doi.org/10.1364/OE.26.004448
18. X. Liu, X. J. Shen, T. Rui, L. He, B. Zhou, and N. Zheng, "Adiabatic nonlinear optical frequency conversion based on the electro-optic effect", Optics Letters, 45, 467 (2020). DOI: https://doi.org/10.1364/OL.377024
19. P. Zhang, J. Cheng, Y. Wu, R. Yan, R. Zhu, T. Wang, L. Jiang, C. Tong, and Y. Song, "Frequency tripled semiconductor disk laser with over 0.5 W ultraviolet output power", Optics Express, 32, 5011 (2024). DOI: https://doi.org/10.1364/OE.514322
20. E. Simonova, A. Kokh, V. Shevchenko, A. Kuznetsov, A. Kragzhda, and P. Fedorov, "Growth of β-BaB_2O_4 Crystals from Solution in LiF–NaF Melt and Study of Phase Equilibria", Crystal Research and Technology, 54, 1800267 (2019). DOI: https://doi.org/10.1002/crat.201800267
21. R. Murai, T. Fukuhara, G. Ando, Y. Tanaka, Y. Takahashi, K. Matsumoto, H. Adachi, M. Maruyama, M. Imanishi, K. Kato, M. Nakajima, Y. Mori, and M. Yoshimura, "Growth of large and high quality $CsLiB_6O_{10}$ crystals from self-flux solutions for high resistance against UV laser-induced degradation", Applied Physics Express, 12, 075501 (2019). DOI: https://dx.doi.org/10.7567/1882-0786/ab25aa

https://doi.org/10.1017/hpl.2024.90 Published online by Cambridge University Press

22. Y. Orii, K. Kohno, H. Tanaka, M. Yoshimura, Y. Mori, J. Nishimae, and K. Shibuya, "Stable 10,000-hour operation of 20-W deep ultraviolet laser generation at 266 nm", Optics Express, 30, 11797 (2022). DOI: https://doi.org/10.1364/OE.454643
23. Z. Hu, Y. Zhao, Y. Yue, and X. Yu, "Large LBO crystal growth at 2 kg-level", Journal of Crystal Growth, 335, 133 (2011). DOI: https://doi.org/10.1016/j.jcrysgro.2011.09.011
24. N. Wang, J. Zhang, H. Yu, X. Lin, and G. Yang, "Sum-frequency generation of 133 mJ, 270 ps laser pulses at 266 nm in LBO crystals", Optics Express, 30, 5700 (2022). DOI: https://doi.org/10.1364/OE.451262
25. H. Yuan, Y. Li, Z. Dan, S. Zhang, and C. Zhu, "Investigation and analysis of pin-point damage and damage growth characteristics in KDP and DKDP crystals", Optics Express, 31, 35786 (2023). DOI: https://doi.org/10.1364/OE.501162
26. Z. Cui, L. Han, C. Wang, M. Sun, D. Liu, and J. Zhu, "Noncritical phase-matching fourth- and fifth-harmonic generation of 1077 nm laser using KDP-family crystals", Optics Letters, 47, 2947 (2022). DOI: https://doi.org/10.1364/OL.458952
27. H. Qi, Z. Wang, F. Yu, X. Sun, X. Xu, and X. Zhao, "Cascaded third-harmonic generation with one KDP crystal", Optics Letters, 41, 5823 (2016). DOI: https://doi.org/10.1364/OL.41.005823
28. H. Yang, D. Li, C. Song, and W. Cheng, "Efficient third-harmonic generation of broadband picosecond radiation by employing spectrally noncritical phase-matching KDP crystal and cascaded LBO crystals", Optics & Laser Technology, 141, 107105 (2021). DOI: https://doi.org/10.1016/j.optlastec.2021.107105
29. G. Hao, M. Xu, X. Sun, B. Liu, L. Zhang, H. Ren, J. Bai, and J. Gao, "Rapid Growth of the Gradient Deuterium Deuterated Potassium Dihydrogen Phosphate Crystal", Crystal Growth & Design, 24, 567 (2023). DOI: https://doi.org/10.1021/acs.cgd.3c01278
30. G. Porat, and A. Arie, "Efficient, broadband, and robust frequency conversion by fully nonlinear adiabatic three-wave mixing," Journal of the Optical Society of America B, 30, 1342 (2013). DOI: https://doi.org/10.1364/JOSAB.30.001342
31. H. Suchowski, B. D. Bruner, A. Ganany-Padowicz, I. Juwiler, A. Arie, and Y. Silberberg, "Adiabatic frequency conversion of ultrafast pulses", Applied Physics B, 105, 697 (2011). DOI: https://doi.org/10.1007/s00340-011-4591-3

32. H. Suchowski, P. R. Krogen, S. W. Huang, F. X. Kärtner, and J. Moses, "Octave-spanning coherent mid-IR generation via adiabatic difference frequency conversion", Optics Express, 21, 28892 (2013). DOI: https://doi.org/10.1364/OE.21.028892
33. L. Ji, X. Zhao, D. Liu, Y. Gao, Y. Cui, D. Rao, W. Feng, F. Li, H. Shi, J. Liu, X. Li, L. Xia, T. Wang, J. Liu, P. Du, X. Sun, W. Ma, Z. Sui, and X. Chen, "High-efficiency second-harmonic generation of low-temporal-coherent light pulse", Optics Letters, 44, 4359 (2019). DOI: https://doi.org/10.1364/OL.44.004359
34. Y. Cui, Y. Gao, D. Rao, D. Liu, F. Li, L. Ji, H. Shi, J. Liu, X. Zhao, W. Feng, L. Xia, J. Liu, X. Li, T. Wang, W. Ma, and Z. Sui, "High-energy low-temporal-coherence instantaneous broadband pulse system", Optics Letters, 44, 2859 (2019). DOI: https://doi.org/10.1364/OL.44.002859
35. X. Zhao, L. Ji, D. Liu, Y. Gao, D. Rao, Y. Cui, W. Feng, F. Li, H. Shi, C. Shan, W. Ma, and Z. Sui, "Second-harmonic generation of temporally low-coherence light", Applied Physics Letters Photonics, 5, 091301 (2020). DOI: https://doi.org/10.1063/5.0022307
36. Z. Sui, and K. Lan, "Driver at 10 MJ and 1 shot/30 min for inertial confinement fusion at high gain: Efficient, compact, low-cost, low laser-plasma instabilities, beam color selectable from 2ω/3ω/4ω, applicable to multiple laser fusion schemes", Matter and Radiation at Extremes, 9, 4 (2024). DOI: https://doi.org/10.48550/arXiv.2405.09912
37. J. E. Midwinter, and J. Warner, "The effects of phase matching method and of uniaxial crystal symmetry on the polar distribution of second-order non-linear optical polarization", British Journal of Applied Physics, 16, 1135 (1965). DOI: https://dx.doi.org/10.1088/0508-3443/16/8/312
38. I. Shoji, T. Kondo, A. Kitamoto, M. Shirane, and R. Ito, "Absolute scale of second-order nonlinear-optical coefficients", Journal of the Optical Society of America B, 14, 2268 (1997). DOI: https://doi.org/10.1364/JOSAB.14.002268
39. Y. Chen, P. Yuan, L. Qian, H. Zhu, and D. Fan, "Numerical study on the efficient generation of 351 nm broadband pulses by frequency mixing of broadband and narrowband Nd: glass lasers," Optics Communications, 283, 2737 (2010). DOI: https://doi.org/10.1016/j.optcom.2010.03.008

https://doi.org/10.1017/hpl.2024.90 Published online by Cambridge University Press

40. H. Zhong, P. Yuan, S. Wen, and L. Qian, “Temperature-insensitive frequency tripling for generating high-average power UV lasers”, Optics Express, 22, 4267 (2014). DOI: https://doi.org/10.1364/OE.22.004267
41. Y. Chen, P. Yuan, and L. Qian, “A broadband frequency-tripling scheme for an Nd: glass laser-based chirped-pulse amplification system: an approach for efficiently generating ultraviolet petawatt pulses,” Journal of Optics, 13, 075205 (2011). DOI: https://dx.doi.org/10.1088/2040-8978/13/7/075205

https://doi.org/10.1017/hpl.2024.90 Published online by Cambridge University Press